Enhanced Photocatalytic Hydrogen Production over Graphene Oxide–Cadmium Sulfide Nanocomposite under Visible Light Irradiation

ARTICLE *in* THE JOURNAL OF PHYSICAL CHEMISTRY C · OCTOBER 2012

Impact Factor: 4.77 · DOI: 10.1021/jp306947d

5 AUTHORS, INCLUDING:

Tianyou Peng
Wuhan University
214 PUBLICATIONS **5,214** CITATIONS

THE JOURNAL OF PHYSICAL CHEMISTRY C

Article

pubs.acs.org/JPCC

Enhanced Photocatalytic Hydrogen Production over Graphene Oxide–Cadmium Sulfide Nanocomposite under Visible Light Irradiation

Tianyou Peng,* Kan Li, Peng Zeng, Qinggang Zhang, and Xungao Zhang*

College of Chemistry and Molecular Science, Wuhan University, Wuhan 430072, P. R. China

ABSTRACT: A series of graphene oxide (GO)–cadmium sulfide (CdS) nanocomposites were fabricated via a facile precipitation process by using $Cd(Ac)_2$, Na_2S, and prefabricated GO as raw materials. The obtained GO–CdS nanocomposites are composed of CdS nanoparticles with an average diameter of ca.10 nm, which are well dispersed and immobilized on GO sheets. By using Na_2S/Na_2SO_3 as sacrificial reagent, the GO–CdS nanocomposites exhibit higher photoactivity for hydrogen production than the bare CdS under visible-light irradiation. Among various composite photocatalysts prepared, 5 wt % GO–CdS shows maximum hydrogen production efficiency. Our findings demonstrate that the coupled GO can serve as CdS supporting matrix, cocatalyst, and electron acceptor for effective charge separation, and therefore provide an inexpensive means to achieve high-performance visible-light-driven photocatalysts for hydrogen production without noble metal-loading.

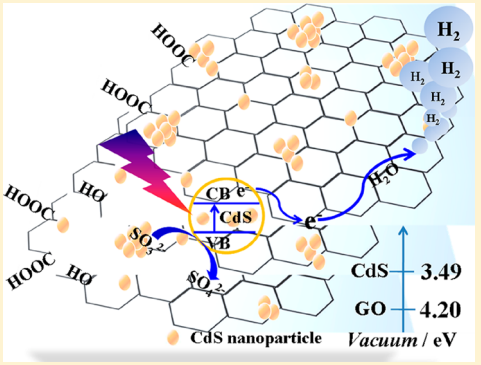

1. INTRODUCTION

Hydrogen (H_2) has been identified as a promising energy carrier due to its high energy capacity and environmental friendliness. Therefore, as a potential direct production routine of clean hydrogen energy, photocatalytic H_2 production over semiconductor has attracted extensive attention during the past decades.[1,2] However, most oxide semiconductors such as TiO_2 mainly absorb UV-light that only takes up ca. 4% of the solar energy, resulting in low light utilization efficiency and even the overall process being impractical.[1−3] However, cadmium sulfide (CdS), as an n-type semiconductor with a bandgap of ∼2.42 eV, has a high visible-light-driven photoactivity for H_2 production.[3] Nevertheless, CdS is prone to photocorrosion during the photoreaction where CdS is itself oxidized by the photogenerated holes,[2] hence some reducing reagents (such as, S^{2-}, SO_3^{2-}, or $S_2O_3^{2-}$) have been applied to stabilize the CdS nanoparticles in a photocatalytic system.[3−6] It has also been reported that mesoporous silica can be used as a support to improve the photostability of the loaded CdS nanoparticles.[4] Moreover, coupling with other wide bandgap semiconductors with suitable bandgap structure can provide an interface for the charge transfer, and then improve the photoactivity for H_2 production of CdS.[6] Also, noble metals such as Pt, Pd, and Rh are generally loaded on TiO_2 or CdS as cocatalysts to provide active sites for the photoreaction and to suppress the charge recombination processes.[1,2] Unfortunately, noble metals possess the disadvantages of being rare and expensive, which limit their wide application. Therefore, the development of photocatalysts with high visible-light-responsive activity and stability for cheap and efficient H_2 production is currently an intensive research topic.[1−6]

Since its discovery in 2004,[7] graphene (G) and/or graphene oxide (GO) have gained a lot of attention due to its excellent physical, chemical, photoelectric, and catalytic properties.[8−10] GO is a complex system consisting of graphene sheets covalently bonded to oxygen-containing functional groups like hydroxyl and epoxy groups on the basal planes and carbonyl/carboxylic acid at the edges.[11−13] Unlike graphite, however, GO is easy to exfoliate and disperse in aqueous solution like wrinkled paper because the oxygen-containing groups are hydrophilic.[11−18] Therefore, GO is usually used as starting materials to prepare graphene (G) or reduced graphene oxide (RGO) by using $NaBH_4$ or hydrazine as reducer.[11−17] Generally, the bandgap energy of GO depends on the number of oxygenated sites and oxidization degree of graphene.[11,14,18] The conduction band (CB) edge of GO, which is mainly formed by the antibonding π^* orbital, has a higher energy level than that needed for H_2 generation, thus leading to electron injection into the solution phase for H_2 generation.[18] However, the valence band (VB) edge mainly contains the O2p orbital and bonding π orbital. Namely, fully oxidized GO is an insulator because of the composition of the oxygen bonding that forms the sp^3 hybridization on graphene, while partially oxidized GO and graphene are a semiconductor and a conductor, respectively.[17] For example, Yan et al.[18] reported that the bandgap of GO can be modulated from 4.0 eV down to 0.1 eV by controlling its oxygenated sites and oxidization level based on the first-principle calculations.[14] Yeh et al.[18] synthesized a moderately oxidized graphite oxide with apparent

Received: July 12, 2012
Revised: October 5, 2012
Published: October 17, 2012

dx.doi.org/10.1021/jp306947d | J. Phys. Chem. C 2012, 116, 22720−22726

bandgap of 2.4−4.3 eV, which showed photocatalytic H_2 production from an aqueous solution containing methanol as sacrificial reagent. Although the apparent quantum yield (AQY) is very low (only 0.01%) under visible-light irradiation, this result illustrated the potential of GO as a photocatalyst for H_2 production.

However, the flat two-dimensional (2D) structure and chemical and physical features of GO make it not only an excellent supporting matrix to anchor CdS nanoparticles and suppress its growth but also an electron acceptor to effectively inhibit the charge recombination.[8−10,19] Therefore, coupling of GO with CdS is expected to improve the performance of CdS. With this in mind, several strategies have been developed for fabrication of GO (or G)−CdS composite.[19,20] For example, Li et al.[20] used 0.5 wt % Pt-loaded CdS-cluster-decorated graphene as photocatalyst for H_2 production, and an apparent quantum yield (AQY) of 22.5% at 420 nm light irradiation was obtained. In addition to acting as the supporting matrix and electron acceptor, GO (or G) also has potential as a cocatalyst in a CdS-based composite for steady H_2 evolution without noble metal-loading because the lowest energy level of GO's CB (the antibonding π^* orbital) is higher than that needed for H_2 generation as mentioned above.[11,14,18] To the best of our knowledge, however, to date, only a few investigations have concerned GO (or G)−CdS composite regarding the application of its cocatalyst property for photocatalytic H_2 production without noble metal-loading.[21−23] For example, it was found that the nitrogen-doped graphene (N-graphene) in a N-graphene/CdS nanocomposite acted as cocatalyst and protective layer that can prevent CdS from photocorrosion, therefore resulting in much higher visible-light-driven photoactivity for H_2 production than the sole CdS.[21] RGO−CdS nanocomposite was also prepared by a one-pot solvothermal process in our group;[22] it exhibited higher photoactivity for H_2 production without noble metal-loading than the bare CdS. Very recently, modified graphene (mG)−CdS composite was fabricated via an electrostatic assembly process and also displayed high photoactivity for H_2 production, which compares favorably with the H_2 production efficiency of Pt-loaded systems under the same conditions.[23]

The above results demonstrated that the coupled 2D carbonaceous material (such as GO, RGO, or G) in the CdS-based composites can serve as not only supporting matrix and the electron acceptor but also as an inexpensive cocatalyst for effective photocatalytic H_2 production. Herein, a series of GO−CdS nanocomposites were fabricated by a facile precipitation process. The obtained products without noble metal-loading were used as photocatalyst for H_2 production under visible-light irradiation by using Na_2S/Na_2SO_3 as sacrificial reagent, and the effects of GO content in the composite on the crystal structure, optical property, and photoactivity for H_2 production were also investigated in detail. Furthermore, a possible mechanism for the photocatalytic reaction in the GO−CdS system is proposed.

2. EXPERIMENTAL SECTION

2.1. Materials Preparation. Graphene oxide (GO) was synthesized by a modified Hummers' method.[24] Typically, 5.0 g of graphite powder and 2.5 g of $NaNO_3$ were added to 115 mL of concentrated H_2SO_4 in an ice-bath, and then 15.0 g of $KMnO_4$ was added gradually under stirring. The mixture was stirred at 35 °C for 4h, and then 230 mL of distilled water was added to the mixture, followed by stirring the resultant mixture at 98 °C for 15 min. The suspension was further diluted to 700 mL and stirred for 30 min. The reaction was terminated by adding 12 mL of H_2O_2 (35 wt %) under stirring. The resulting solids were separated and washed with water and acetone, and then dried at 40 °C overnight to obtain the graphite oxide (GTO).[24] The obtained GTO (0.5 g) was dispersed in 100 mL water and treated for 1 h by ultrasonic waves. After centrifugation (3000 rpm) for 10 min, the sample was frozen and then warmed in a vacuum to obtain the exfoliated GO.

GO−CdS was prepared by a method similar to the electrostatic assembly process of mG−CdS reported by Lv et al.[23] Typically, 2.66 g of $Cd(Ac)_2{\cdot}2H_2O$ and 76 mg of exfoliated GO were added to 100 mL of water to obtain 0.1 M $Cd(Ac)_2$ solution, and then 100 mL of Na_2S solution (0.11 M) was added dropwise under stirring. The resultant mixture was continuously stirred for 1 h. After centrifugation, the product was washed with water and acetone and then dried at 40 °C overnight to obtain 5 wt % GO−CdS nanocomposites. By varying the GO addition amount, GO−CdS nanocomposites with different GO addition levels were prepared. Moreover, the above procedure was repeated in the absence of GO to obtain the bare CdS nanoparticles as control.

2.2. Materials Characterization. Raman spectra were detected by a Laser Confocal Raman Microspectroscopy (Hpriba Jobin Yvon LabRAM HR 800 UV) using the 632.8 nm line of an argon ion laser as the excitation source. X-ray photoelectron spectra (XPS) were recorded on a Kratos XSAM800 X-ray photoelectron spectroscope equipped with a standard and monochromatic source (MgKα) operated at 150 W (15 kV, 10 mA). Powder X-ray diffraction (XRD) patterns were obtained on a Bruker D8 advance X-ray diffractometer with CuKα radiation (λ = 0.15418 nm) at 40 kV and 100 mA. Transmission electron microscopy (TEM) images were obtained on a LaB6 JEM-2010(HT)-FEF electron microscope. Photoluminescence spectra were obtained on a F4500 fluorometer (Hitachi). The diffuse reflectance absorption spectra (DRS) were recorded on a Cary 5000 UV−vis-NIR spectrophotometer equipped with an integrating sphere by using $BaSO_4$ as a reference.

2.3. Evaluation of Photocatalytic Activity. Photocatalytic reactions were carried out in an outer irradiation-type photoreactor (pyrex glass) containing an aqueous solution of 0.35 M Na_2S and 0.25 M Na_2SO_3 (100 mL) as sacrificial reagent. A 300 W Xe-lamp (PLS-SXE300, Beijing Trusttech Co. Ltd.) was employed as the light source as described elsewhere.[6] A cutoff filter (Kenko L-42, $\lambda \geq 420$ nm) was used for visible-light irradiation. Before the light irradiation, the photoreactor containing photocatalyst and sacrificial reagent solution was treated for 15 min by ultrasonic waves to let the photocatalyst be dispersed uniformly, and then thoroughly degassed to remove air. The evolved H_2 amount was determined by a gas chromatograph (GC, SP-6800A, thermal conductivity detector, 5 Å molecular sieve columns, and Ar carrier).

To evaluate the photostability, the photocatalyst after the first run of 5 h photochemical reaction was separated from the suspension, washed with water, and dried at 70 °C, and then, the recovered photocatalyst was used for the second and third run of the photoreaction under the same conditions. The apparent quantum yield (AQY) was measured under the same photoreaction conditions, except for the incident light wavelength. The hydrogen yields of 1 h photoreaction under different light wavelengths (420, 450, 475, 500, 520, and 550 nm) were measured. The band-pass and cutoff filters and a

dx.doi.org/10.1021/jp306947d | J. Phys. Chem. C 2012, 116, 22720−22726

calibrated Si-photodiode (SRC-1000-TC-QZ-N, Oriel) were used in the measurement. AQY values at different incident light wavelengths were calculated by the following equation:[1,6]

$$\mathrm{AQY}(\%) = \frac{\text{number of reacted electrons}}{\text{number of incident photons}} \times 100$$

$$= \frac{2 \times \text{number of evolved } H_2 \text{ molecules}}{\text{number of incident photons}} \times 100$$

3. RESULTS AND DISCUSSION

3.1. Crystal Phase and Raman Spectrum Analyses. Figure 1 shows the XRD patterns of the pristine graphite (PG),

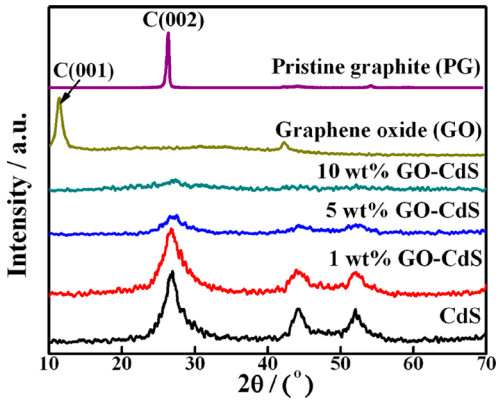

Figure 1. XRD patterns of PG, GO, and CdS and GO−CdS nanocomposites with different GO addition levels.

graphene oxide (GO), CdS, and GO−CdS nanocomposites with different GO addition levels. The sharp (002) diffraction peak of PG at 2θ = ~26.3° indicates the characteristic interlayer distance of ~0.34 nm,[10,18] while GO shows no graphitic diffraction peak but a broader characteristic peak at a lower diffraction angle (2θ = ~11.3°), corresponding to the (001) reflection peak with an interlayer distance of ~0.8 nm, which is similar to the previously reported values.[8,10,18] The disappearance of the characteristic (002) reflection of PG confirms that oxidization took place, resulting in the formation of GO with well-defined lamellar structure.[10,18] The enhanced interlayer distance of GO is related to the existence of oxygen-containing functional groups and to the changes in the carbon hexahedron grid plane during the present oxidization and exfoliation processes.[18,20,21]

The bare CdS shows three broad peaks located at 2θ = 26.9°, 44.2°, and 52.0°, ascribable to the (111), (220), and (311) planes of the cubic CdS (JCPDS 42-1411).[10,23] The diffraction peak intensities of CdS in the composite gradually decrease upon enhancing the GO addition level, which is similar to the previous observation.[10] Once the GO addition level reaches 10 wt %, the obviously depressed diffraction peak intensities make the composite similar to an amorphous structure, indicating that GO can successfully immobilize CdS nanoparticles on its surface and retard the crystallite growth.[10,23] It can be validated by the fact that the average crystal size (~3 nm) of CdS in 5 wt % GO−CdS is smaller than that (~4.8 nm) of the bare CdS as calculated from the peak broadening by using the Scherrer equation. Moreover, diffraction peaks of GO are not observed even from the XRD pattern of 10 wt % GO−CdS, indicating complete exfoliation of GO during the ultrasonication of the GTO and the followed preparation processes of the composite.[10,23]

Raman spectra in Figure 2 show that the major peaks of PG are G-band at ~1580 cm^{-1}, D-band at ~1340 cm^{-1}, and 2D-

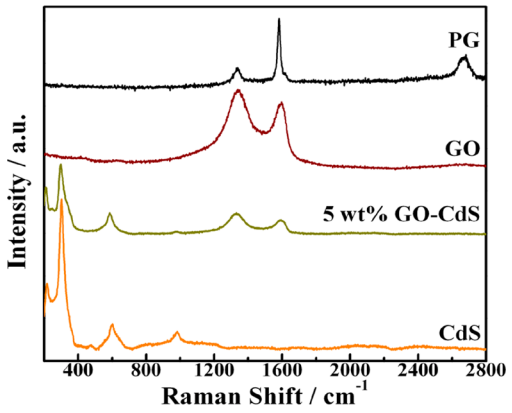

Figure 2. Raman spectra of PG, GO, CdS, and 5 wt % GO−CdS nanocomposite.

band at ~2678 cm^{-1}, respectively.[12,25] The G-band (graphite carbon band) originates from in-plane vibration of sp^2 carbon atoms, and the 2D-band is a doubly degenerate (TO and LO) phonon mode (E_{2g} symmetry) at the Brillouin zone center.[12,25] It has been reported that the D-band (disordered carbon band) due to the first-order zone boundary phonons is absent from a defect-free graphene but exists in a defected graphene.[25] After the oxidation process, the defect-induced D-band at ~1340 cm^{-1} markedly increased, indicating that the layer-stacking regularity was disrupted and defects were introduced.[12,25] The longitudinal optical (LO) phonon peaks of 5 wt % GO−CdS are seen at ca. 302, 598 (second order), and 984 cm^{-1} (third order) for the CdS in the composite.[22,23] The intensity of D/G ratio of GO in the composite shown in Figure 2 is almost similar to the bare GO, demonstrating that there exists a nondestructive coalescent approach during the formation of GO−CdS nanocomposite.[12,22,23]

3.2. Microstructure and Composition Analyses. The morphologies of the bare GO, CdS, and 5 wt % GO−CdS can be observed from Figure 3. There are few GO layers (Figure 3a), which are typically well spread out and curved, with a wrinkled morphology due to the presence of the functional groups and the extremely small thickness. Direct evidence for the immobilization of CdS nanoparticles on GO sheets can be observed from the HRTEM image (Figure 3b). Most of CdS nanoparticles with average size of ca. 10 nm are well dispersed and immobilized on the GO surface. The inset in Figure 3b indicates that the CdS nanoparticles in GO−CdS have high crystallinity with a well-resolved lattice spacing of ca. 0.34 nm. The diameter of the CdS particles in GO−CdS is smaller than that of the bare aggregated CdS nanoparticles (Figure 3c). This may be attributed to the interaction between CdS and GO with −COOH and −OH groups that can stabilize the CdS surfaces and retard the aggregation and growth of CdS nanoparticle.[23]

In order to better understand the chemical composition of the prepared composite, energy dispersive X-ray (EDX) spectrum of GO−CdS was recorded and shown in Figure 3d. As can be seen, there exists the signals of cadmium, sulfur, and carbon elements with a weight ratio of CdS/C = 96.4:3.6, which was approximate to the initial addition amount. X-ray

dx.doi.org/10.1021/jp306947d | J. Phys. Chem. C 2012, 116, 22720−22726

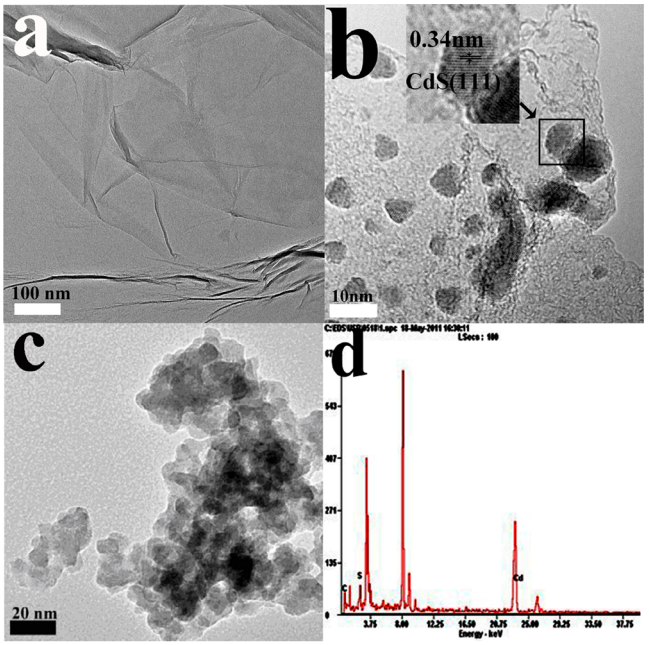

Figure 3. TEM images of GO (a), 5 wt % GO−CdS nanocomposite (b), and CdS (c); EDX spectrum (d) of 5 wt % GO−CdS nanocomposite.

photoelectron spectroscopy (XPS) is a surface analytical technique that can provide useful information on the nature of the functional groups and also on the chemical composition of surfaces. Full XPS spectrum of 5 wt % CdS−GO is shown in Figure 4a. The existence of C1s, S2p, Cd3d, and O1s in the composite can be clearly observed. The C1s spectrum (Figure 4b) of the composite can be deconvoluted into four peaks. The main peak of C1s located at 284.6 eV is attributed to the sp^2 bonded carbon in the graphitic structure, whereas the other three peaks at 285.6, 286.7, and 288.6 eV are assigned to carbon atoms in hydroxyls (C−O), epoxy (C−O), and carboxyl (O═C−OH) functional groups, respectively.[9,10] Compared with the bare GO (Figure 4c), the intensity of the C−O and C═O peaks in composite is dramatically decreased, indicating the partial removal of the oxygen-containing functional groups.[20] These results are consistent with the above XRD, TEM, EDX, and Raman analyses, which further confirm the complete exfoliation and partial reduction of GO, and the covalent attachment of the CdS to the GO surfaces during the preparation process.[8,10]

3.3. UV−Vis Diffuse Reflectance Absorption Spectra Analyses. Figure 5 shows the UV−vis diffuse reflectance absorption spectra (DRS) of the bare GO, CdS, and GO−CdS nanocomposites with different GO addition levels. As can be seen, the absorption onset for the bare CdS is ~580 nm,

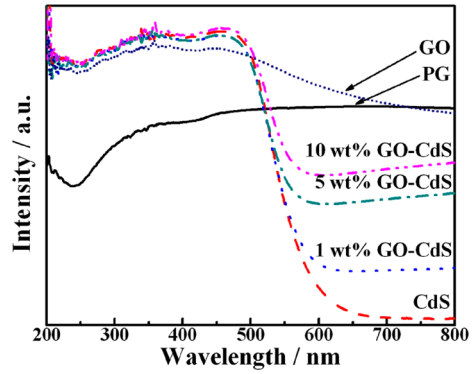

Figure 5. UV−vis diffuse reflectance absorption spectra (DRS) of GO, CdS, and GO−CdS nanocomposites with different GO addition levels.

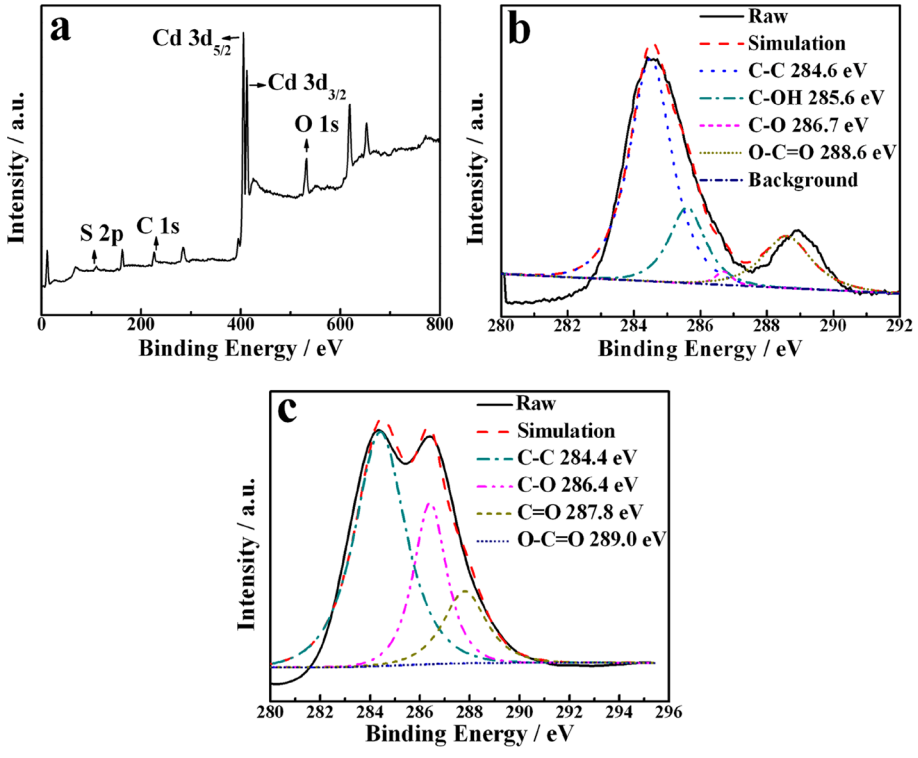

Figure 4. XPS spectrum of 5 wt % GO−CdS (a); high-resolution XPS spectra of GO−CdS (b) and bare GO (c).

dx.doi.org/10.1021/jp306947d | J. Phys. Chem. C 2012, 116, 22720−22726

corresponding to the bandgap of ~2.14 eV, which is much smaller than that (2.42 eV) of the bulk CdS. It indicates their different physical properties (such as smaller particle size and more detects) stemming from the different preparation processes,[22] which can also be validated by the TEM observation (Figure 3b). The bare GO shows excellent light absorption in the range of 200−800 nm and a unconspicuous absorption onset at ca. 750 nm, which is similar to the previous observation.[18,22] Theoretical bandgap structure analyses showed that the gap nature of graphene changes from direct to indirect with increasing oxidation level.[18] This is related to a change of the highest VB band state from the bonding π orbital to the O2p orbital. However, the present GO does not show a sharp adsorption edge for a precise gap energy because GO is not a crystal and is made of graphene molecules containing different oxidation levels. From an approximate estimation based on the absorption onset at ca. 750 nm, the apparent bandgap of the present GO is ca. 1.65 eV, which is much smaller than the reported values (2.4−4.3 eV) of graphite oxide.[18] Considering, the more $\pi \rightarrow \pi^*$ transitions, the less energythat needs to be used for the electronic transition, which can result in an adsorption edge with higher wavelength.[18] The above small bandgap of the present GO possibly implies a low oxidization degree of graphene during the preparation process.

Although CdS has no absorption above its fundamental absorption edge rising at ~580 nm, the composites show a broad elevated background in the visible region due to the presence of GO.[23] Moreover, there is an enhanced absorbance in the visible-light region (>580 nm) with increasing the GO content. This can also be observed from the color change of the samples, which become darker with increasing the GO content. It could be attributed to the enhancement of the surface electric charge of the CdS in the composite because of the introduction of GO, which leads to the possible electronic transition of $\pi \rightarrow \pi^*$ of GO and $n \rightarrow \pi^*$ between the n-orbital of the sulfur species in CdS and GO.[6] This enhancement happens at wavelength longer than 580 nm, indicating that a more efficient utilization of the solar energy can be obtained. Therefore, it can be inferred that the introduction of GO in CdS particles would have influence on the fundamental process of the photogenerated carrier formation and separation in the photocatalytic process.

3.4. Photocatalytic H_2 Production Efficiency and Stability. Control experiments show no appreciable H_2 evolution in the absence of either photocatalyst or light irradiation. Photocatalytic H_2 production rates from various product suspensions containing Na_2SO_3 (0.25 M)−Na_2S (0.35 M) solution under visible-light ($\lambda \geq 420$ nm) irradiation are shown in Figure 6. GO demonstrates a limited amount of H_2 evolution with a rate of only ~4 μmol h^{-1}, which is similar to the previous report that partially oxidized graphite oxide showed an AQY of 0.01% for H_2 evolution from an aqueous solution containing methanol as sacificial reagent under visible-light irradiation.[18] The low H_2 evolution efficiency indicates that GO with this oxidation level was not effective for energy conversion by absorbing visible light. It should be noted that the above H_2 production does not require noble metal as cocatalyst because the lowest energy level of the CB (antibonding π^* orbital) of GO is higher than that needed for H_2 generation as reported previously.[18] The above positive response to visible-light irradiation reflects the potential of GO as a photocatalyst and/or cocatalyst (in a composite system) for steady H_2 evolution without noble metal-loading although

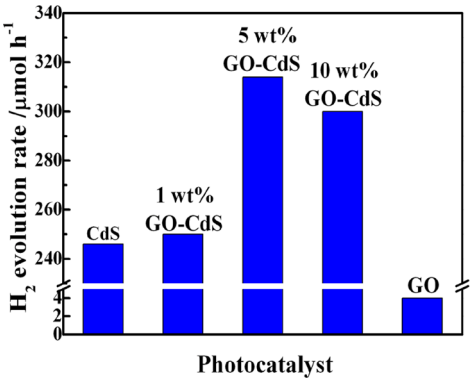

Figure 6. Photocatalytic H_2 production rates over various samples. Conditions: 100 mg of catalysts, 100 mL of Na_2S (0.35 M)−Na_2SO_3 (0.25 M) solution, 300 W Xe-lamp equipped with cutoff filter ($\lambda \geq$ 420 nm), irradiation 2 h.

further investigation is necessary for unstanding the more detailed correlation between the GO bandgap and the oxidation level of graphene sheets.

As can be seen from Figure 6, the bare CdS demonstrates 246 μmol h^{-1} of H_2 evolution rate under visible-light irradiation, which could be ascribed to its narrow bandgap (ca. 2.14 eV) as mentioned above. After coupling with GO, the photocatalytic H_2 production rate is improved at different extents as compared to the bare CdS. The H_2 evolution rate increases with increasing GO-loading up to 5 wt % and then decreases at a higher GO-loading. Namely, 5 wt % GO−CdS composite shows a maximum H_2 production rate (314 μmol h^{-1}). On one hand, GO has a 2D carbon-based ideal molecular structure, in which electrons can be considered to move freely, so it can act as good electron acceptors. Lv et al.[23] reported that graphene behaved in a manner similar to Pt, accepting and transferring electrons and acting as an effective H_2 evolution promoter for CdS.[23] It is thus reasonable to draw the conclusion that an efficient photoinduced charge transfer occurs between the CdS and the GO, and then resulting in the enhanced H_2 production efficiencies of the composites with GO content smaller than 5 wt %. On the other hand, the decrease in photocatalytic efficiencies at higher GO-loading levels may result from the excessive GO shielding CdS from the incident light.[23] Another possible reason may be ascribed to the presence of GO that leads to the decreases in the relative amount of CdS and then to the decrease of the photogenerated carriers because the same amount of photocatalyst (100 mg) was used for the photoreaction.

Typical time courses for H_2 production over various photocatalysts are presented in Figure 7. As can be seen, the H_2 production rate of the bare CdS is lower than 5 wt % GO−CdS, indicating that the distinctive structure of GO is critical for the photogenerated carrier separation. The repeated experiments of GO−CdS were conducted in three consecutive runs, accumulating 15 h with fresh sacrificial reagent solution periodically replaced in each run. In a control experiment, poor photocatalytic efficiency was observed when methanol was employed as sacrificial reagent in the same photoreaction system, indicating that the Na_2S−Na_2SO_3 mixture is also a crucial factor for the photoreaction, which could enhance photocatalytic performance and suppress the photocorrosion. Five wt % GO−CdS displays photoactivity with an average H_2 generation of 314 μmol h^{-1} in the first run of 5 h photoreaction, and maintains relatively steady H_2 generation

dx.doi.org/10.1021/jp306947d | J. Phys. Chem. C 2012, 116, 22720−22726

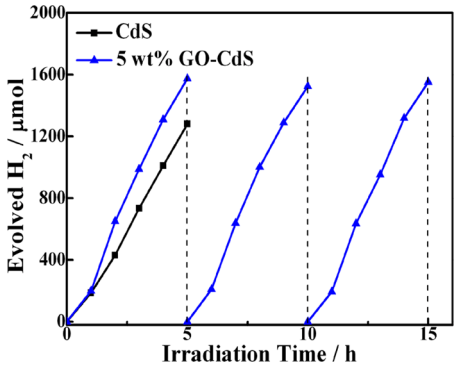

Figure 7. Time courses for photocatalytic H_2 evolution over various samples. Conditions: 100 mg of catalysts, 100 mL of Na_2S (0.35 M)−Na_2SO_3 (0.25 M) solution, 300 W Xe-lamp equipped with cutoff filter ($\lambda \geq 420$ nm).

rates of 305 and 315 μmol h^{-1} in the second and third run of 5 h photoreaction, respectively. It indicates that the photocorrosion of CdS in the present nanocomposite is very limited.

3.5. Discussion on the Photocatalytic H_2 Production Mechanism. The AQY for H_2 production over 5 wt % GO−CdS reaches a maximum of 4.8% under 420 nm monochromatic light irradiation as shown in Figure 8. It can be

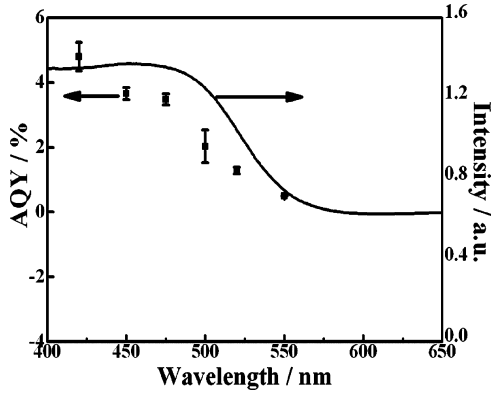

Figure 8. Comparison of DRS spectrum and apparent quantum yield of 5 wt % GO−CdS (100 mg) in 100 mL of Na_2SO_3 (0.25 M)−Na_2S (0.35 M) aqueous suspension.

observed that AQY value decreases with increasing the incident light wavelength, which is consistent with the change tendency of DRS spectrum as shown in Figure 8. The longest wavelength suitable for H_2 evolution was found to coincide with the absorption edge of the bare CdS even though the composite still shows high absorbance at wavelength > 580 nm, indicating that the H_2 evolution reaction was indeed driven by the photoinduced CdS excitation, and the light absorption property of CdS in composite governed the photoactivity for H_2 production. Therefore, the relative energetics should be considered for H_2 production over the present composite. It has been reported that the CB energy level of CdS is ca. 3.49 eV,[5] whereas the work function of GO is ca. 4.20 eV,[26] suggesting that the photogenerated electron transferring from the CB of CdS to GO is thermodynamically allowed.

On the basis of the above results and discussions, a possible mechanism for photocatalytic H_2 production over the GO−CdS was proposed as illustrated in Figure 9. The energy level of GO is lower than the CB of CdS and higher than the water

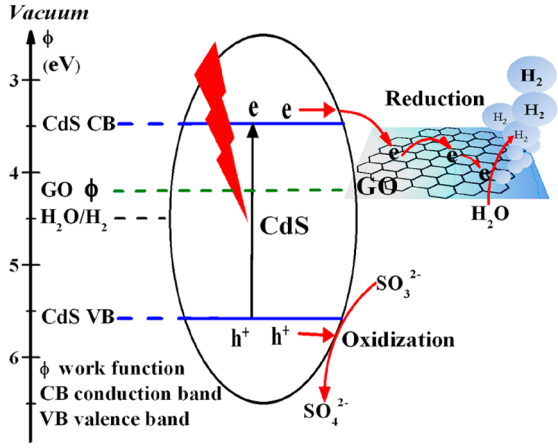

Figure 9. Diagram of the proposed mechanism for the photocatalytic H_2 production in the present system.

reduction potential;[23,26] therefore, the photoexcited electrons in the CB of CdS can be captured by the GO and transferred quickly to carbon atoms on the GO sheets, which are accessible to the adsorbed H^+ ions (from water ionization) to produce H_2. The sacrificial reagent will complement the electrons to the remaining holes in the VB of CdS. To further confirm the above assumption, photoluminescence (PL) properties of the obtained samples were investigated as shown in Figure 10. It

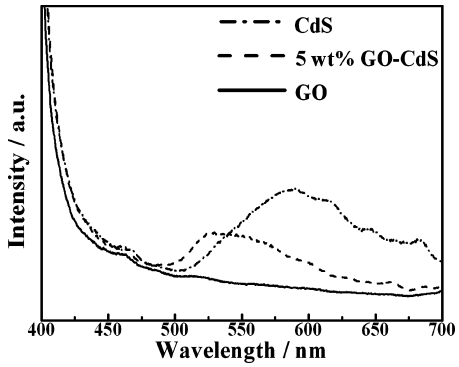

Figure 10. PL spectra of GO, CdS, and 5 wt % GO−CdS with an excitation wavelength of 380 nm.

can be clearly seen that the bare CdS exhibiting a strong broad peak located at ca. 580 nm, which locates near the absorption edge, may be attributed to surface defects and vacancies of the nanoparticles.[8,9,23] In addition, almost no emission could be directly observed from GO, and significant fluorescence quenching of CdS can be observed after coupling CdS with GO. It indicates that the electron−hole pairs in the excited CdS could be efficiently separated and that the electrons efficiently transfer from the CdS to the GO sheet.

In fact, many photoelectrochemical measurements confirmed that GO as electron acceptor can improved electron transfer properties.[23,27−29] For example, Lv et al.[23] demonstrated that graphene attached to semiconductor can efficiently accept electrons from the excited semiconductor and suppress the charge recombination by using time-resolved emission spectra and photocurrent generated response measurement techniques. Li et al.[27] studied the photocurrent generation capability and the incident photon to current conversion efficiency of graphene−CdS, and the improvement of efficiency was ascribed

dx.doi.org/10.1021/jp306947d | J. Phys. Chem. C 2012, 116, 22720−22726

to the unique sheet morphology and the electronic property of graphene. Cao et al.[29] found that the graphene−CdS has lower time constants due to the electron transfer from the excited CdS to the graphene by employing time-resolved fluorescence spectroscopy. Wang et al.[9] also revealed that graphene has a high ability to accept electrons by using transient photovoltage technique. Therefore, it can be concluded that coupling GO with the CdS can increase the electron acceptance and transport rate in the composite and then suppress the charge recombination; thereby, a higher efficiency could be achieved. Apparently, the above results suggested interesting possibility for the preparation of efficient carbon-based composite photocatalyst with better durability and broader light absorption range in comparison to the bare CdS. The interfacial combination between the two components is helpful to hinder the backward electron transfer and improve the electron injection and quantum efficiency. By the present facile process, the unique properties of GO can be utilized by coupling with not only CdS but also other semiconductors, which provides an inexpensive means of harnessing solar energy and an efficient photocatalyst for H_2 production.

4. CONCLUSIONS

In summary, a series of GO−CdS nanocomposites were successfully fabricated though a facile precipitation process and structurally characterized. The obtained composites show enhanced photocatalytic performance as compared to the bare CdS under the same conditions, and 5 wt % GO−CdS reaches a maximum H_2 evolution rate of 314 μmol h^{-1} under visible-light irradiation. GO coupled with the CdS nanoparticles can efficiently accept and transport electrons from the excited semiconductor, which is beneficial for suppressing the charge recombination and then for improving the interfacial charge transfer processes and the photocatalytic activity for H_2 production. The present investigation seems to highlight the most interesting possibility, namely, utilizing the unique properties of GO as cocatalyst, electron acceptor, and supporting matrix by appropriate designing of graphitic material, which is cheap, abundant, and environmentally friendly, to develop cheap, efficient photocatalysts for H_2 production with durable and steady characteristics.

AUTHOR INFORMATION

Corresponding Author

*Tel/Fax: +86-27 6875 2237. E-mail: typeng@whu.edu.cn (T.P.); xgzhang@whu.edu.cn (X.Z.).

Notes

The authors declare no competing financial interest.

ACKNOWLEDGMENTS

This work was supported by the Natural Science Foundation of China (20973128 and 21271146), the Program for New Century Excellent Talents in University (NCET-07-0637), and Independence Innovation Program (2081003) of Wuhan University, China. We also gratefully thank Dr. Ying Liu for XPS analysis and helpful discussion.

REFERENCES

(1) Kudo, A.; Miseki, Y. *Chem. Soc. Rev.* **2009**, *38*, 253−278.
(2) Chen, X. B.; Shen, S. H.; Guo, L. J.; Mao, S. S. *Chem. Rev.* **2010**, *110*, 6503−6570.
(3) Xing, C. J.; Zhang, Y. J.; Yan, W.; Guo, L. J. *Int. J. Hydrogen Energy* **2006**, *31*, 2018−2024.
(4) Ryu, S. Y.; Balcerski, W.; Lee, T. K.; Hoffmann, M. R. *J. Phys. Chem. C* **2007**, *111*, 18195−18203.
(5) Kim, Y. K.; Park, H. *Energy Environ Sci.* **2011**, *4*, 685−694.
(6) Liu, X. J.; Zeng, P.; Peng, T. Y.; Zhang, C. H.; Deng, K. J. *Int. J. Hydrogen Energy* **2012**, *37*, 1375−1384.
(7) Novoselov, K. S.; Geim, A. K.; Morozov, S. V.; Jiang, D.; Zhang, Y.; Dubonos, S. V.; Grigorieva, I. V.; Firsov, A. A. *Science* **2004**, *306*, 666−667.
(8) Nethravathi, C.; Nisha, T.; Ravishankar, N.; Shivakumara, C.; Rajamathi, M. *Carbon* **2009**, *47*, 2054−2059.
(9) Wang, P.; Jiang, T. F.; Zhu, C. Z.; Zhai, Y. M.; Wang, D. J.; Dong, S. J. *Nano Res.* **2010**, *3*, 794−799.
(10) Pham, T. A.; Choi, B. C.; Jeong, Y. T. *Nanotechnology* **2010**, *21*, 465603.
(11) Mathkar, A.; Tozier, D.; Cox, P.; Ong, P.; Galande, C.; Balakrishnan, K.; Reddy, A. L. M.; Ajayan, P. M. *J. Phys. Chem. Lett.* **2012**, *3*, 986−991.
(12) Zhu, Y. W.; Murali, S.; Cai, W. W.; Li, X. S.; Suk, J. W.; Potts, J. R.; Ruoff, R. S. *Adv. Mater.* **2010**, *22*, 3906−3924.
(13) Dreyer, D. R.; Park, S.; Bielawski, C. W.; Ruoff, R. S. *Chem. Soc. Rev.* **2010**, *39*, 228−240.
(14) Yan, J. A.; Xian, L. D.; Chou, M. Y. *Phys. Rev. Lett.* **2009**, *103*, 086802.
(15) Geim, A. K. *Science* **2009**, *324*, 1530−1534.
(16) Kamat, P. V. *J. Phys. Chem. Lett.* **2011**, *2*, 242−252.
(17) Zhuo, S. J.; Shao, M. W.; Lee, S. T. *ACS Nano* **2012**, *6*, 1059−1064.
(18) Yeh, T. F.; Syu, J. M.; Cheng, C.; Chang, T. H.; Teng, H. *Adv. Funct. Mater.* **2010**, *20*, 2255−2262.
(19) Shen, L.; Zeng, M. G.; Yang, S. W.; Zhang, C.; Wang, X. F.; Feng, Y. P. *J. Am. Chem. Soc.* **2010**, *132*, 11481−11486.
(20) Li, Q.; Guo, B. D.; Yu, J. G.; Ran, J. R.; Zhang, B. H.; Yan, H. J.; Gong, J. R. *J. Am. Chem. Soc.* **2011**, *133*, 10878−10884.
(21) Jia, L.; Wang, D. H.; Huang, Y. X.; Xu, A. W.; Yu, H. Q. *J. Phys. Chem. C* **2011**, *115*, 11466−11473.
(22) Zeng, P.; Zhang, Q. G.; Peng, T. Y.; Zhang, X. H. *Phys. Chem. Chem. Phys.* **2011**, *13*, 21496−21502.
(23) Lv, X. J.; Fu, W. F.; Chang, H. X.; Zhang, H.; Cheng, J .S.; Zhang, G. J.; Song, Y.; Hu, C. Y.; Li, J. H. *J. Mater. Chem.* **2012**, *22*, 1539−1546.
(24) Hummers, W. S.; Offeman, R. E., Jr. *J. Am. Chem. Soc.* **1958**, *80*, 1339−1340.
(25) Ni, Z. H.; Wang, Y. Y.; Yu, T.; Shen, Z. X. *Nano Res.* **2008**, *1*, 273−291.
(26) Shin, H. J.; Kim, K. K.; Benayad, A.; Yoon, S. M.; Park, H. K.; Jung, S. I.; Jin, M. H.; Jeong, H. K.; Kim, J. M.; Choi, J. Y.; et al. *Adv. Funct. Mater.* **2009**, *19*, 1987−1992.
(27) Chang, H. V.; Lv, X. J.; Zhang, H.; Li, J. H. *Electrochem. Commun.* **2010**, *12*, 483−487.
(28) Guo, Y. S.; Jia, X. P.; Zhang, S. S. *Chem. Commun.* **2011**, *47*, 725−727.
(29) Cao, A. N.; Liu, Z.; Chu, S. S.; Wu, M. H.; Ye, Z. M.; Cai, Z. W.; Chang, Y. L.; Wang, S. F.; Gong, Q. H.; Liu, Y. F. *Adv. Mater.* **2010**, *22*, 103−106.